

Vibration-Tolerant Hall-Effect Transmission Speed and Direction Sensor IC

FEATURES AND BENEFITS

- **Differential Hall-effect sensor IC** measures ring magnets and ferrous targets with inherent stray field immunity
- **Vibration detection algorithms** prevent false switching and provide low-signal lockout
- **Large operating air gap** with independent switch points
- **Three-wire pulse-width output protocol** describes speed and direction
- **Wide operating voltage** and integrated protection circuits
- **AEC-Q100 Grade 0 qualified** for an ambient operating temperature range of -40°C to 150°C

PACKAGE: 4-PIN SIP (SUFFIX K)



Not to scale

DESCRIPTION

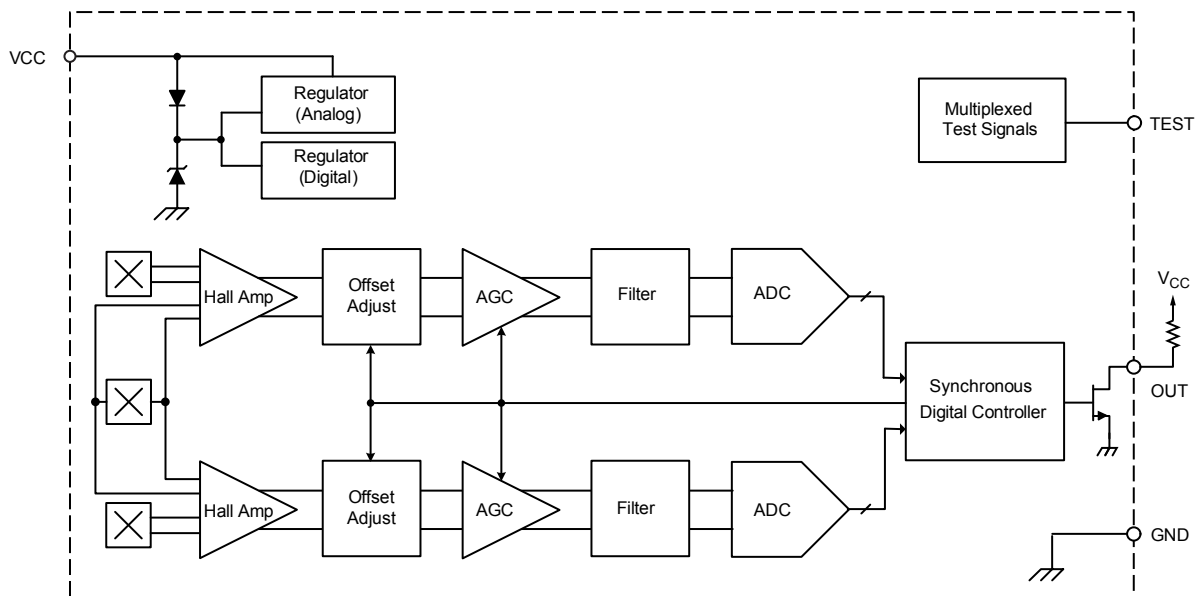
The A1693 is a magnetic sensor IC designed for measuring the speed and direction of rotating transmission systems. This IC can directly measure ring magnets or be back-biased with a magnet to measure ferrous targets.

The IC incorporates three Hall-effect elements that sense differentially, analog signal conditioning with dynamic gain and offset adjustment, analog-to-digital converters (ADCs), and a digital processor that applies intelligent algorithms to prevent the output from switching when the sensed target vibrates.

The A1693 output is an open collector that requires a pull-up resistor. Each time a new magnetic state is detected, the output goes low for a pulse-width time that communicates a forward-direction, reverse-direction, or non-direction.

The sensor IC is AEC-Q100 qualified for automotive applications, and is provided in a lead (Pb) free 4-pin single inline package (SIP) with 100% matte tin leadframe plating.

Functional Block Diagram



A1693

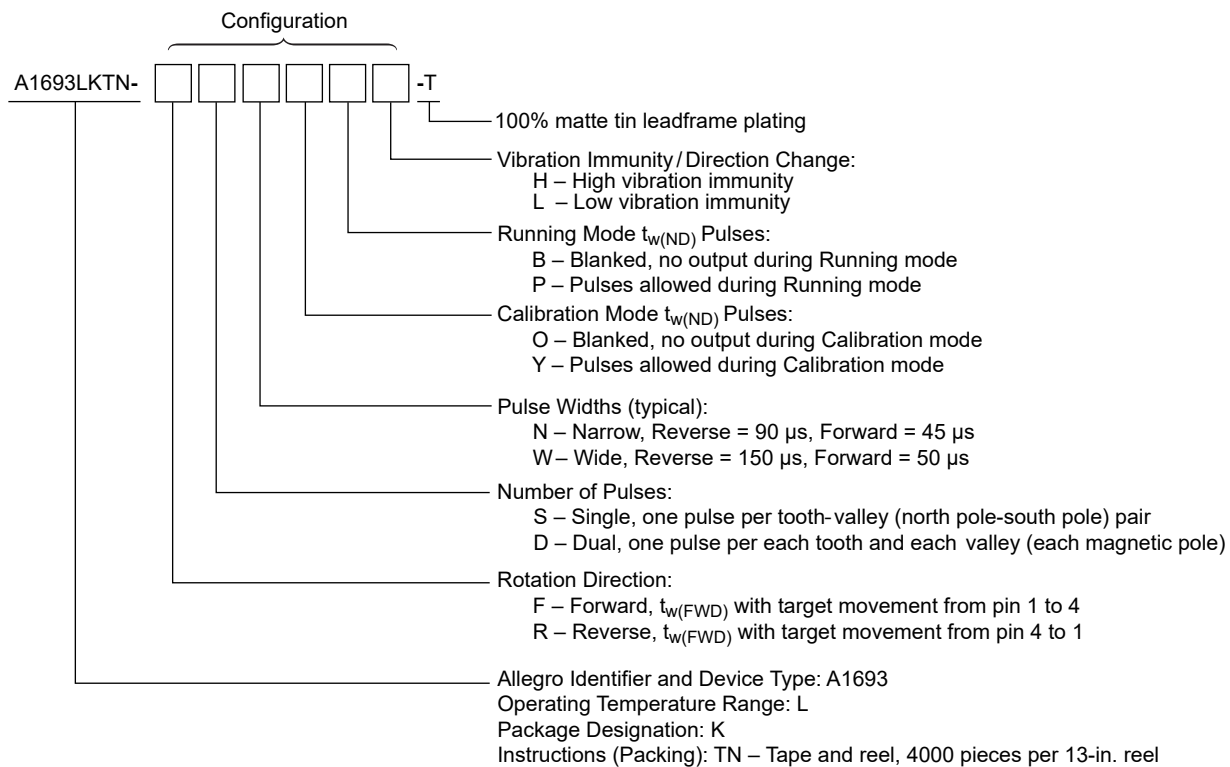
Vibration-Tolerant Hall-Effect Transmission Speed and Direction Sensor IC

SELECTION GUIDE

Part Number*	Package	Packing
A1693LKTN-RSNOBH-T	4-pin SIP	4000 pieces per 13-inch reel



* Not all combinations are available. Contact Allegro for availability and pricing of custom programming or packing options.

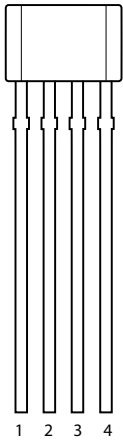


All variants: Target configuration is ring magnet, device should be back-biased for ferromagnetic target operation.

ABSOLUTE MAXIMUM RATINGS

Characteristic	Symbol	Notes	Rating	Unit
Supply Voltage	V_{CC}	Refer to Power Derating section	28	V
Reverse Supply Voltage	V_{RCC}		-18	V
Reverse Output Voltage	V_{ROUT}		-0.5	V
Output Sink Current	I_{OUT}		25	mA
Operating Ambient Temperature	T_A	L temperature range	-40 to 150	°C
Maximum Junction Temperature	$T_{J(max)}$		165	°C
Storage Temperature	T_{stg}		-65 to 170	°C

Pinout Diagram



Terminal List Table

Number	Name	Function
1	VCC	Supply voltage
2	OUT	Open collector output
3	TEST	Test pin: float *
4	GND	Ground

*Connection of TEST to VCC and/or GND may cause undesired additional current consumption in the IC.

OPERATING CHARACTERISTICS: Valid throughout full operating and temperature ranges, unless otherwise specified

Characteristic	Symbol	Test Conditions	Min.	Typ. [1]	Max.	Unit [2]
GENERAL ELECTRICAL CHARACTERISTICS						
Supply Voltage [3]	V_{CC}	Operating, $T_J < T_{J(max)}$	4	–	24	V
Under Voltage Lockout	$V_{CC(UV)}$	$V_{CC} 0 \rightarrow 5\text{ V}$ or $5 \rightarrow 0\text{ V}$	–	3.6	3.95	V
Reverse Supply Current [4]	I_{RCC}	$V_{CC} = V_{RCC(max)}$	–10	–	–	mA
Supply Zener Clamp Voltage	$V_{Z(SUPPLY)}$	$I_{CC} = I_{CC(max)} + 3\text{ mA}$, $T_A = 25^\circ\text{C}$	28	–	–	V
Supply Current	I_{CC}		5	–	12	mA
Test Pin Zener Clamp Voltage [5]	$V_{Z(TEST)}$		–	6	–	V
Power-On State	POS	Output, when connected as in Figure 10	–	High	–	–
Output Rise Time	t_r	$R_{PULLUP} = 825\ \Omega$, $C_{LOAD} = 4.7\text{ nF}$, 10% to 90%, connected as in Figure 10	–	10	–	μs
Output Fall Time	t_f	$R_{PULLUP} = 825\ \Omega$, $C_{LOAD} = 4.7\text{ nF}$, 90% to 10%, connected as in Figure 10	–	0.9	–	μs
OUTPUT STAGE						
Low Output Voltage	$V_{OUT(sat)}$	$I_{SINK} = 10\text{ mA}$, Output = On	–	200	500	mV
Output Zener Clamp Voltage	V_{ZOUT}		26.5	–	–	V
Output Current Limit	I_{lim}	$V_{OUT} = 12\text{ V}$, $T_J < T_{J(max)}$	25	45	70	mA
Output Leakage Current	I_{OFF}	Output = Off, $V_{OUT} = 24\text{ V}$	–	–	10	μA
OUTPUT PULSE CHARACTERISTICS [6]						
Pulse Width (Forward Rotation)	$t_{w(FWD)}$	N (Narrow) option	38	45	52	μs
		W (Wide) option	42	50	58	μs
Pulse Width (Reverse Rotation)	$t_{w(REV)}$	N (Narrow) option	76	90	104	μs
		W (Wide) option	127	150	173	μs
Pulse Width (Non-Direction)	$t_{w(ND)}$	N (Narrow) option	306	360	414	μs
GENERAL OPERATING CHARACTERISTICS						
Operate Point	B_{OP}	% of peak-to-peak IC-processed signal	–	69	–	%
Release Point	B_{RP}	% of peak-to-peak IC-processed signal	–	31	–	%
Operating Frequency (Forward Rotation) [7][8]	f_{FWD}	S (Single) option	0	–	11.1	kHz
		D (Dual) option	0	–	5.6	kHz
Operating Frequency (Reverse Rotation) [7][8]	f_{REV}	NS (Narrow, Single) options	0	–	7	kHz
		ND (Narrow, Dual) options	0	–	3.5	kHz
		WS (Wide, Single) options	0	–	4.7	kHz
		WD (Wide, Dual) options	0	–	3.5	kHz
Operating Frequency (Non-Direction Pulses) [7][8]	f_{ND}	S (Single) option	0	–	2.2	kHz
		D (Dual) option	0	–	1.1	kHz
DAC CHARACTERISTICS						
Allowable User-Induced Offset	B_{OFFSET}	Magnitude valid for both differential magnetic channels	–300	–	300	G

Continued on the next page...

OPERATING CHARACTERISTICS (continued): Valid throughout full operating and temperature ranges, unless otherwise specified

Characteristic	Symbol	Test Conditions	Min.	Typ. [1]	Max.	Unit [2]	
PERFORMANCE CHARACTERISTICS							
Operating Differential Magnetic Input [9]	$B_{DIFF(pk-pk)}$	Peak to peak differential signal, valid for each magnetic channel	30	–	1200	G	
Vibration Immunity (Startup)	$err_{VIB(SU)}$	Option H, see Figure 1	T_{CYCLE}	–	–	–	
		Option L, see Figure 1	$0.5 \times T_{CYCLE}$	–	–	–	
Vibration Immunity (Running Mode)	err_{VIB}	Option H, see Figure 1	T_{CYCLE}	–	–	–	
		Option L, see Figure 1	$0.5 \times T_{CYCLE}$	–	–	–	
INPUT MAGNETIC CHARACTERISTICS							
Allowable Differential Sequential Signal Variation [10]	$B_{SEQ(n+1)} / B_{SEQ(n)}$	Signal cycle-to-cycle variation (see Figure 3)	0.6	–	–	–	
Switchpoint Separation	$V_{SP(sep)}$	Minimum separation between channels as a percentage of signal amplitude at each switchpoint (see Figure 2)	20	–	–	% pk-pk	
CALIBRATION							
First Direction Output Pulse [11]		Option H: Amount of target rotation (constant direction) following power-on until first electrical output pulse of either $t_{w(FWD)}$ or $t_{w(REV)}$, see Figure 1	$B_{DIFF(pk-pk)} < 1200\text{ G}$ $B_{DIFF(pk-pk)} > 60\text{ G}$	–	$2 \times T_{CYCLE}$	$< 3 \times T_{CYCLE}$	–
			$B_{DIFF(pk-pk)} < 60\text{ G}$ $B_{DIFF(pk-pk)} > 30\text{ G}$	–	$2.5 \times T_{CYCLE}$	$< 4 \times T_{CYCLE}$	–
		Option L: Amount of target rotation (constant direction) following power-on until first electrical output pulse of either $t_{w(FWD)}$ or $t_{w(REV)}$, see Figure 1		–	$1.8 \times T_{CYCLE}$	$2.2 \times T_{CYCLE}$	–
First Direction Pulse Output Following Direction Change	N_{CD}	Option H: Amount of target rotation (constant direction) following event until first electrical output pulse of either $t_{w(FWD)}$ or $t_{w(REV)}$, see Figure 1		$1 \times T_{CYCLE}$	$2 \times T_{CYCLE}$	$< 3 \times T_{CYCLE}$	–
		Option L: Amount of target rotation (constant direction) following event until first electrical output pulse of either $t_{w(FWD)}$ or $t_{w(REV)}$, see Figure 1		–	–	$2 \times T_{CYCLE}$	–
First Direction Pulse Output Following Running Mode Vibration		Option H: Amount of target rotation (constant direction) following event until first electrical output pulse of either $t_{w(FWD)}$ or $t_{w(REV)}$, see Figure 1		$1 \times T_{CYCLE}$	$2 \times T_{CYCLE}$	$< 3 \times T_{CYCLE}$	–
		Option L: Amount of target rotation (constant direction) following event until first electrical output pulse of either $t_{w(FWD)}$ or $t_{w(REV)}$, see Figure 1		–	–	$2 \times T_{CYCLE}$	–

[1] Typical values are at $T_A = 25^\circ\text{C}$ and $V_{CC} = 12\text{ V}$. Performance may vary for individual units, within the specified maximum and minimum limits.

[2] 1 G (gauss) = 0.1 mT (millitesla).

[3] Maximum voltage must be adjusted for power dissipation and junction temperature; see Power Derating section.

[4] Negative current is defined as conventional current coming out of (sourced from) the specified device terminal.

[5] Sustained voltages beyond the clamp voltage may cause permanent damage to the IC.

[6] Load circuit is $C_L = 10\text{ pF}$ and $R_{PULLUP} = 1.2\text{ k}\Omega$. Pulse duration measured at a threshold of $V_{PULLUP} / 2$.

[7] Maximums of both Operating Frequency (Reverse Rotation) and Operating Frequency (Non-Direction Pulses) are determined by satisfactory separation of output pulses: $V_{OUT(HIGH)}$ of $t_{w(FWD)}$ (min). If the customer can resolve shorter high-state durations, maximum f_{REV} and f_{ND} may be increased.

[8] Frequency of T_{CYCLE} .

[9] Differential magnetic field is measured for Channel A (E1-E2) and Channel B (E2-E3) independently. Each channel's differential magnetic field is measured between two Hall elements with spacing shown in package drawing. Magnetic field is measured orthogonally to the front of the package.

[10] If the minimum signal phase separation is not maintained during or after a signal variation event, output may be blanked or non-direction pulses may occur. A signal variation event during power-on may increase the quantity of edges required to get correct direction pulses.

[11] Power-on frequency $\leq 200\text{ Hz}$. Higher power-on frequencies may require more input magnetic cycles until directional output pulses are achieved.

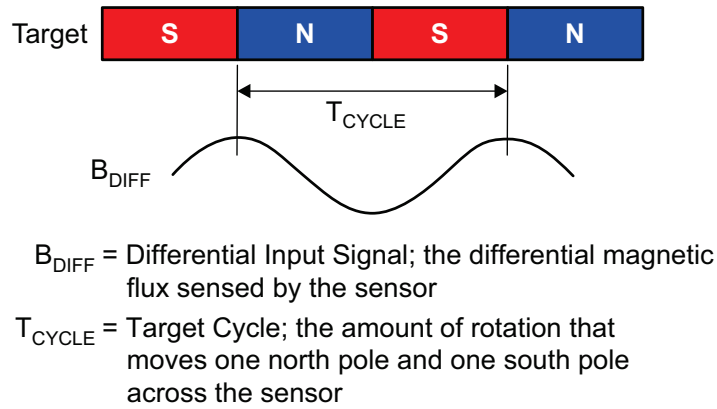


Figure 1: Definition of T_{CYCLE}

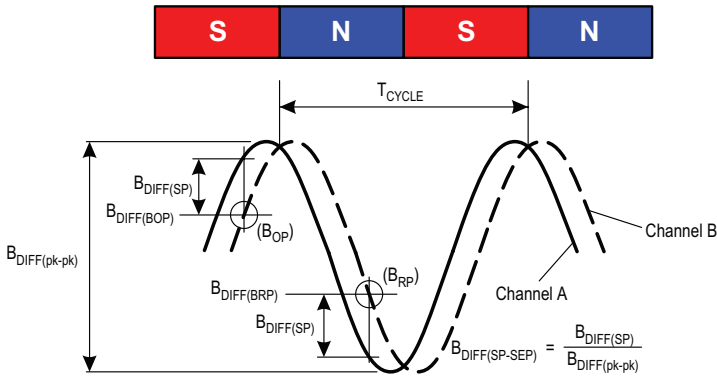


Figure 2: Definition of Switchpoint Separation

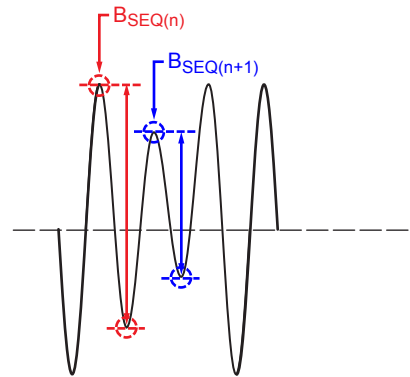
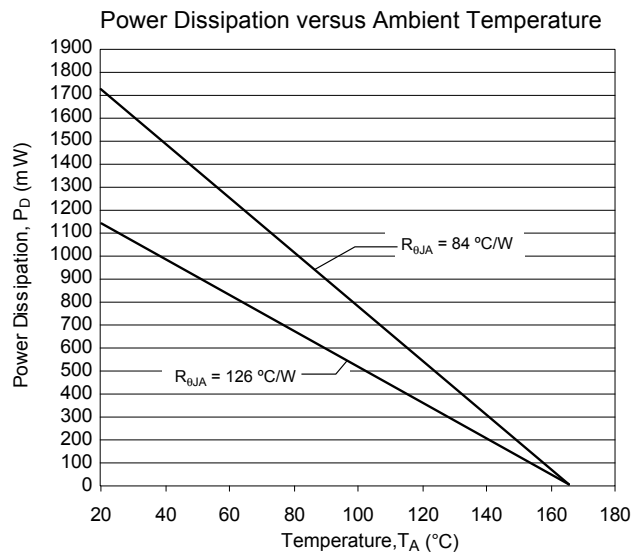
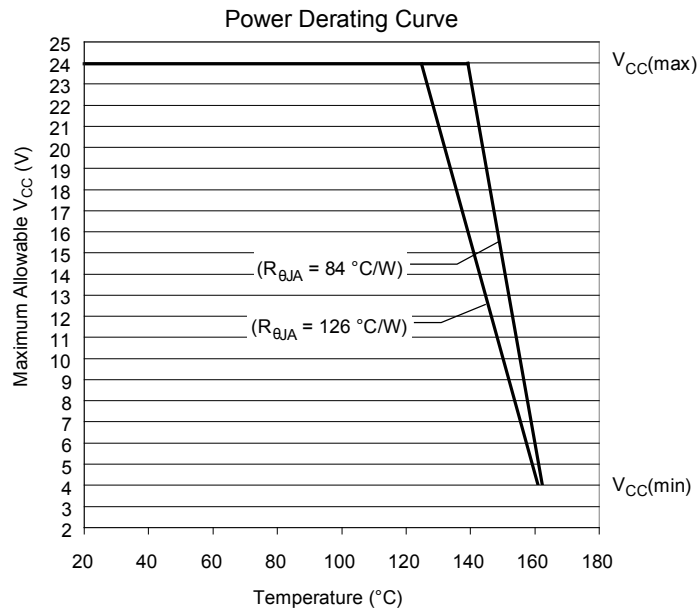


Figure 3: Definition of Differential Signal Variation

THERMAL CHARACTERISTICS: May require derating at maximum conditions; see Power Derating section

Characteristic	Symbol	Test Conditions*	Value	Unit
Package Thermal Resistance	$R_{\theta JA}$	Single layer PCB, with copper limited to solder pads	126	$^{\circ}\text{C}/\text{W}$
		Single layer PCB, with copper limited to solder pads and 3.57 in. ² (23.03 cm ²) copper area each side	84	$^{\circ}\text{C}/\text{W}$

*Additional thermal information available on the Allegro website



FUNCTIONAL DESCRIPTION

Sensing Technology

The sensor IC contains a single-chip Hall-effect circuit that supports a trio of Hall elements. These elements are used in differential pairs to provide electrical signals containing information regarding edge position and direction of target rotation. The A1693 is intended for use with ring magnet targets or, when back-biased with an appropriate magnet, with ferrous targets.

After proper power is applied to the sensor IC, it is capable of providing digital information that is representative of the magnetic features of a rotating target. The waveform diagrams in Figure 5 present the automatic translation of the target profiles, through their induced magnetic profiles, to the digital output signal of the sensor IC.

Direction Detection

The sensor IC compares the relative phase of its two differential channels to determine in which direction the target is moving. The relative switching order is used to determine the direction, which is communicated through the output protocol.

Data Protocol Description

When a target passes in front of the device (opposite the branded face of the package case), the A1693 generates output pulses for features of the target (refer to Timing section). Speed information is provided by the output pulse rate, while direction of target rotation is provided by the duration of the output pulses. The sensor IC can sense target movement in both the forward and reverse directions.

Forward Rotation (see Figure 4): Forward rotation is indicated on the output by a $t_{w(FWD)}$ pulse width. With the -Fxxxx variant, a magnetic pole passing the sensor IC from pin 1 to 4 is defined as forward rotation. With the -Rxxxx variant, forward rotation occurs for target motion from pin 4 to 1.

Reverse Rotation (see Figure 4): Reverse rotation is indicated on the output by a $t_{w(REV)}$ pulse width. With the -Fxxxx variant, a magnetic pole passing the sensor IC from pin 4 to 1 is defined as reverse rotation. With the -Rxxxx variant, reverse rotation occurs for target motion from pin 1 to 4.

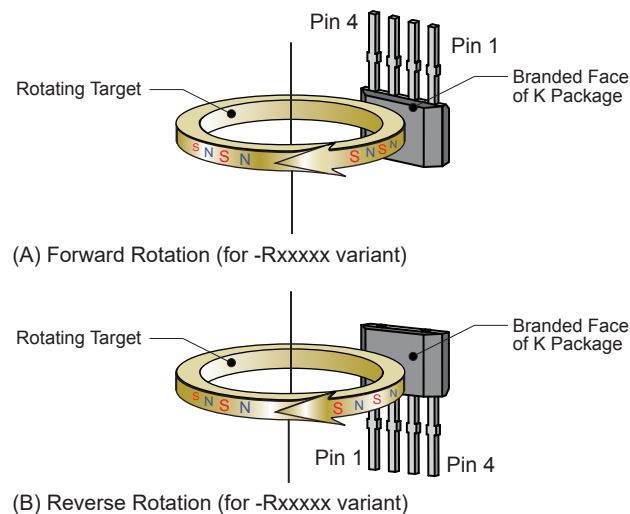
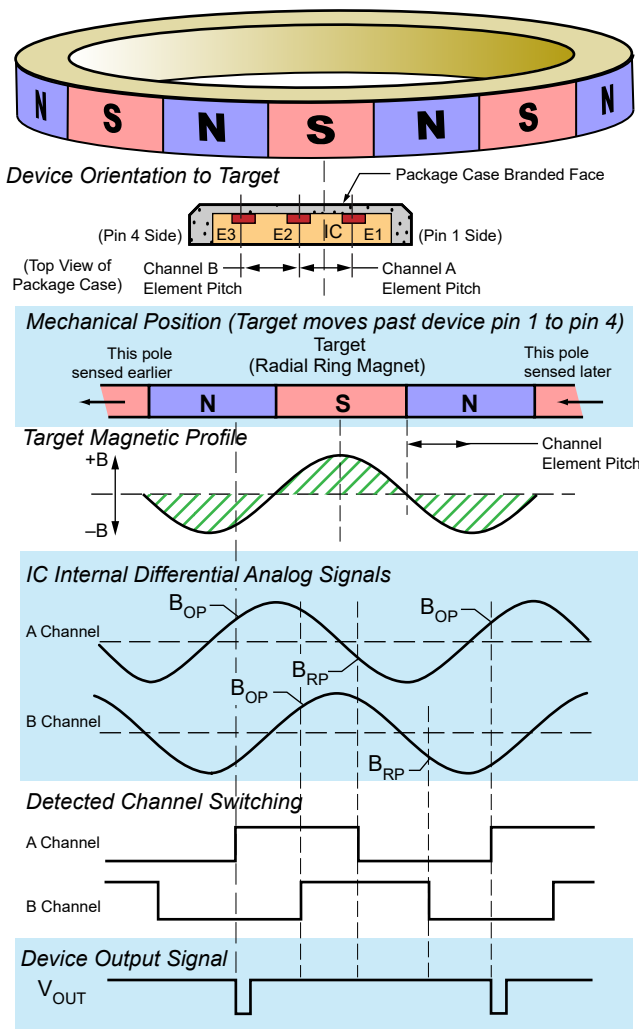
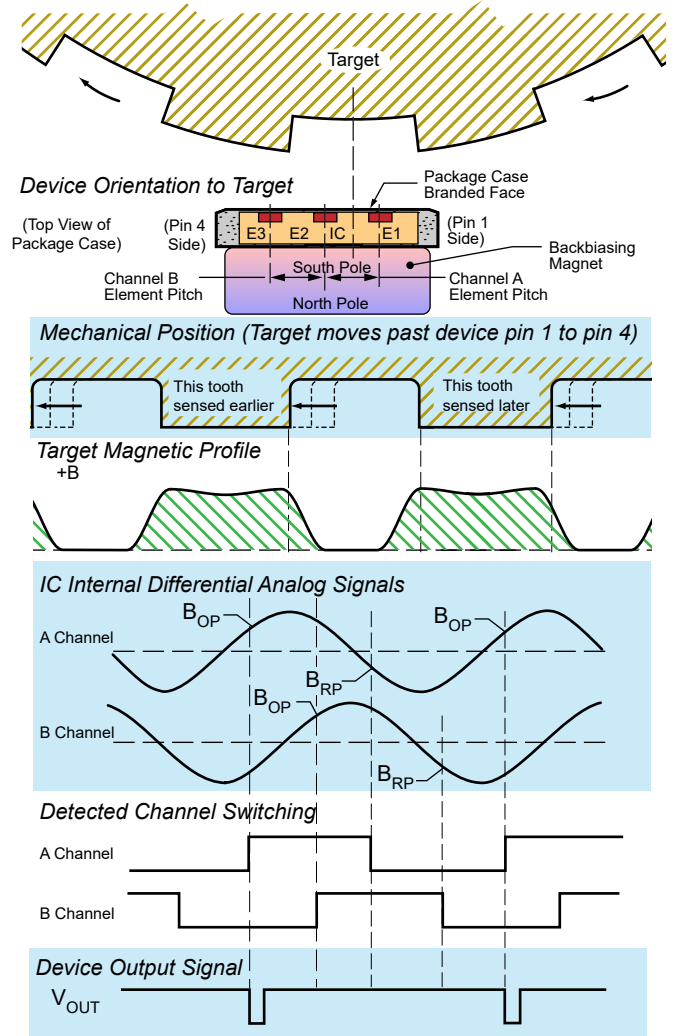


Figure 4: Target Orientation Relative to Device



(A) Ring Magnet Target



(B) Ferromagnetic Target
(with backbiasing magnet)

Figure 5: The magnetic profile reflects the features of the target, allowing the sensor IC to present an accurate digital output. (Option S shown)

Timing As shown in Figure 6, the pulse appears at the output slightly before the sensed magnetic edge traverses the package branded face. With the -FSxxxH option and for targets in forward rotation, this shift, Δf_{wd} , results in the pulse corresponding to the magnetic north region with the sensed magnetic edge, and for targets in reverse rotation, the shift, Δr_{ev} , results in the pulse corresponding to the magnetic south region with the sensed edge. The sensed magnetic edge that stimulates output pulses is kept the same for both forward and reverse rotation by using only one channel to control output switching.

With the -RSxxxH option, the shift direction is inverted and the output pulse occurs on the opposite side of the sensed edge. For targets in forward rotation, this shift, Δf_{wd} , results in the pulse corresponding to the magnetic south region with the sensed magnetic edge, and for targets in reverse rotation, the shift, Δr_{ev} , results in the pulse corresponding to the magnetic north region with the sensed edge.

With the L option, the IC dynamically selects the switchpoint for the output to minimize the calibration duration. Leaving each calibration mode, whether after power-on, direction change, or detected vibration, the IC selects either B_{OP} or B_{RP} from either A or B channel (see Figure 5) as the trigger for the output pulse. Note that for the D option, both B_{OP} and B_{RP} from one channel are used. The switchpoint selection is retained until the next calibration mode is reached, at which point the best switchpoint will again be selected. As a result, the sensed magnetic edge that stimulates output pulses can change, but speed information is not compromised.

Direction Validation

Following a direction change in Running mode, output pulses have a width of $t_{w(ND)}$ until direction information is validated. An example of the waveforms is shown in Figure 7. $t_{w(ND)}$ is not present when using the non-pulse variant (Option B).

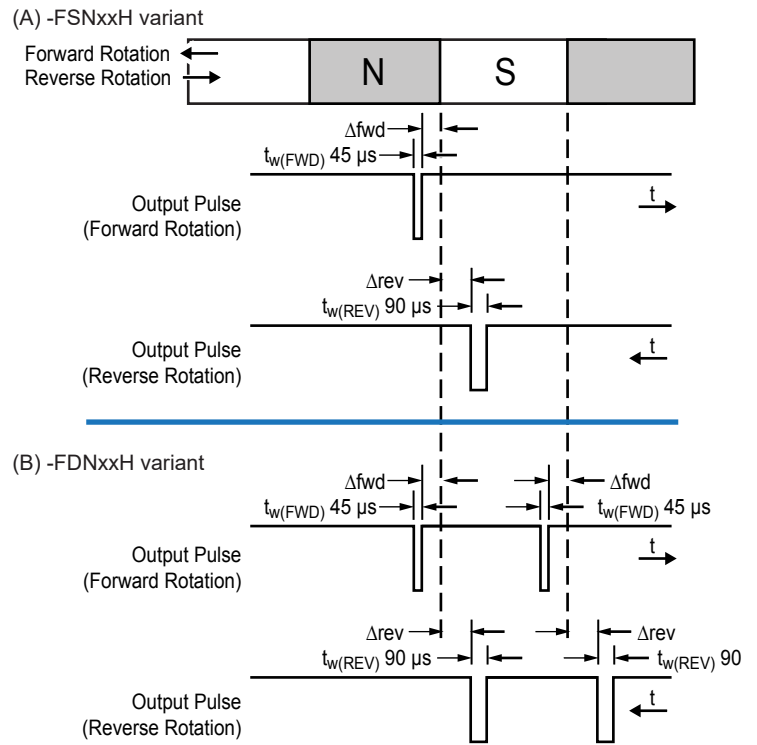


Figure 6: Output Protocol

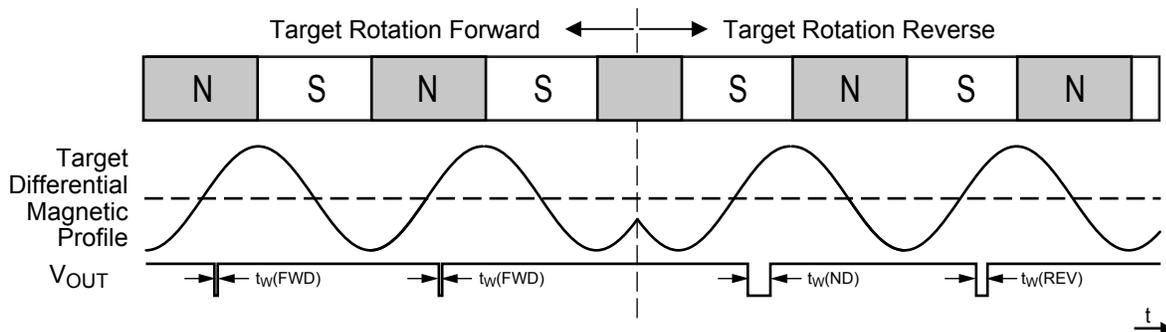


Figure 7: Example of direction change in Running mode F, S, P and H options

Start-Up Detection / Calibration

When power is applied to the A1693, the sensor IC internally detects the profile of the target. The gain and offset of the detected signals are adjusted during the calibration period, normalizing the internal signal amplitude for the air gap range of the device.

The Automatic Gain Control (AGC) feature ensures that operational characteristics are isolated from the effects of installation air gap variation.

Automatic Offset Adjustment (AOA) is circuitry that compensates for the effects of chip, magnet, and installation offsets. This circuitry works with the AGC during calibration to adjust V_{PROC} in the internal A-to-D range to allow for acquisition of signal peaks. AOA and AGC function separately on the two differential signal channels.

Direction information is available after calibration is complete. Figure 8 shows where the first output edges may occur for various starting target phases. $t_{w(ND)}$ pulses are not present with the O variant (Blanked).

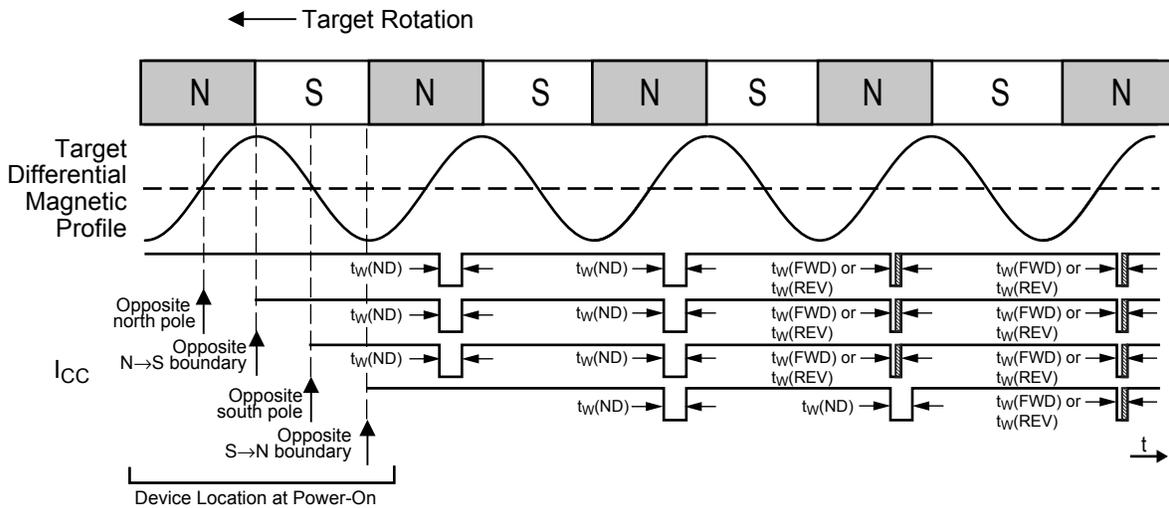


Figure 8: Start-up position effect on first device output switching (Option Y shown: pulse-in-calibration)

Vibration Detection

Algorithms embedded in the IC digital controller detect the presence of target vibration through analysis of the two magnetic input channels.

With the pulses-in-Running mode (Option P) variant, in the presence of vibration, output pulses of $t_{w(ND)}$ may occur or no pulses may occur, depending on the amplitude and phase of the vibration (Figure 9). Output pulses have a width of $t_{w(ND)}$ until direction information is validated on constant target rotation. With the non-pulse (Option B) variant, no $t_{w(ND)}$ pulses will be present.

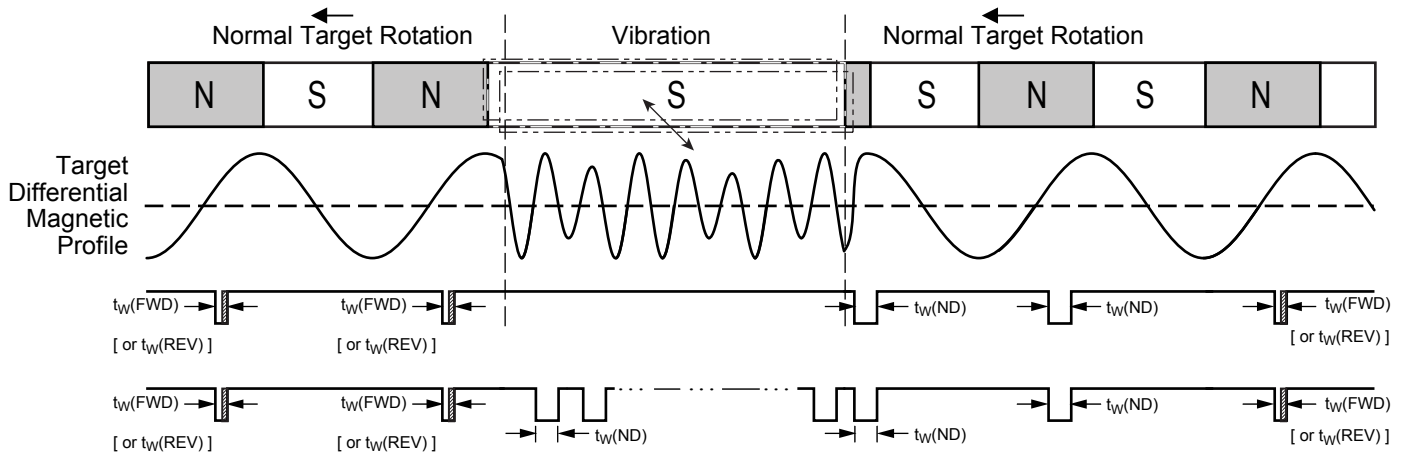


Figure 9: Output functionality in the presence of Running mode target vibration, P option

APPLICATION INFORMATION

Power Derating

The device must be operated below the maximum junction temperature of the device, $T_{J(max)}$. Under certain combinations of peak conditions, reliable operation may require derating supplied power or improving the heat dissipation properties of the application. This section presents a procedure for correlating factors affecting operating T_J . (Thermal data is also available on the Allegro website.)

The Package Thermal Resistance, $R_{\theta JA}$, is a figure of merit summarizing the ability of the application and the device to dissipate heat from the junction (die), through all paths to the ambient air. Its primary component is the Effective Thermal Conductivity, K , of the printed circuit board, including adjacent devices and traces. Radiation from the die through the device case, $R_{\theta JC}$, is relatively small component of $R_{\theta JA}$. Ambient air temperature, T_A , and air motion are significant external factors, damped by overmolding.

The effect of varying power levels (Power Dissipation, P_D), can be estimated. The following formulas represent the fundamental relationships used to estimate T_J , at P_D .

$$P_D = V_{IN} \times I_{IN} \quad (1)$$

$$\Delta T = P_D \times R_{\theta JA} \quad (2)$$

$$T_J = T_A + \Delta T \quad (3)$$

For example, given common conditions such as: $T_A = 25^\circ\text{C}$, $V_{CC} = 12\text{ V}$, $I_{CC} = 6.5\text{ mA}$, and $R_{\theta JA} = 177^\circ\text{C/W}$, then:

$$P_D = V_{CC} \times I_{CC} = 12\text{ V} \times 6.5\text{ mA} = 78\text{ mW}$$

$$\Delta T = P_D \times R_{\theta JA} = 78\text{ mW} \times 177^\circ\text{C/W} = 13.8^\circ\text{C}$$

$$T_J = T_A + \Delta T = 25^\circ\text{C} + 13.8^\circ\text{C} = 38.8^\circ\text{C}$$

A worst-case estimate, $P_D(max)$, represents the maximum allowable power level ($V_{CC(max)}$, $I_{CC(max)}$), without exceeding $T_J(max)$, at a selected $R_{\theta JA}$ and T_A .

Example: Reliability for V_{CC} at $T_A = 150^\circ\text{C}$, package K, using a single-layer PCB.

Observe the worst-case ratings for the device, specifically: $R_{\theta JA} = 177^\circ\text{C/W}$, $T_J(max) = 165^\circ\text{C}$, $V_{CC(max)} = 24\text{ V}$, and $I_{CC(max)} = 12\text{ mA}$.

Calculate the maximum allowable power level, $P_D(max)$. First, invert equation 3:

$$\Delta T_{max} = T_J(max) - T_A = 165^\circ\text{C} - 150^\circ\text{C} = 15^\circ\text{C}$$

This provides the allowable increase to T_J resulting from internal power dissipation. Then, invert equation 2:

$$P_D(max) = \Delta T_{max} \div R_{\theta JA} = 15^\circ\text{C} \div 177^\circ\text{C/W} = 84.7\text{ mW}$$

Finally, invert equation 1 with respect to voltage:

$V_{CC(est)} = P_D(max) \div I_{CC(max)} = 84.7\text{ mW} \div 12\text{ mA} = 7.1\text{ V}$
The result indicates that, at T_A , the application and device can dissipate adequate amounts of heat at voltages $\leq V_{CC(est)}$.

Compare $V_{CC(est)}$ to $V_{CC(max)}$. If $V_{CC(est)} \leq V_{CC(max)}$, then reliable operation between $V_{CC(est)}$ and $V_{CC(max)}$ requires enhanced $R_{\theta JA}$. If $V_{CC(est)} \geq V_{CC(max)}$, then operation between $V_{CC(est)}$ and $V_{CC(max)}$ is reliable under these conditions.

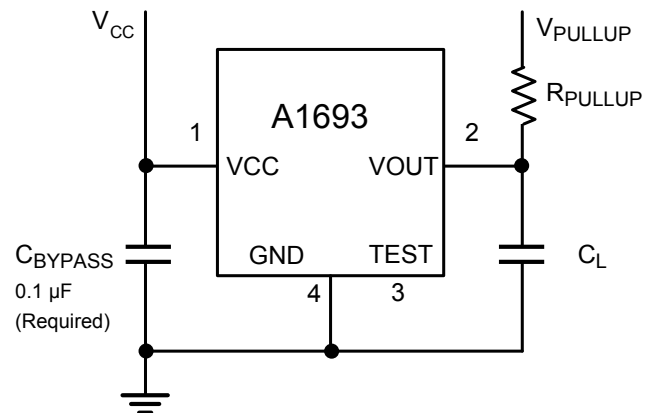
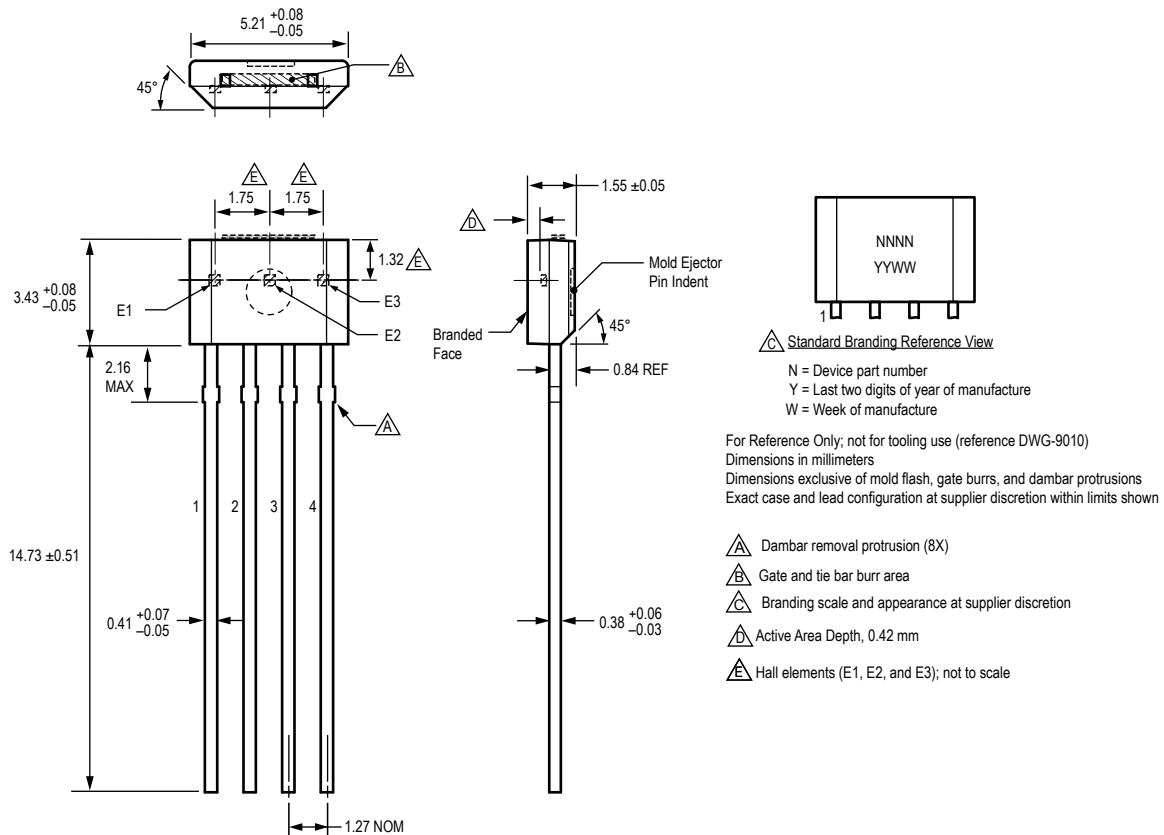


Figure 10: Typical Application Circuit

Package K, 4-Pin SIP



Revision History

Number	Date	Description
–	April 24, 2019	Initial release

Copyright 2019, Allegro MicroSystems.

Allegro MicroSystems reserves the right to make, from time to time, such departures from the detail specifications as may be required to permit improvements in the performance, reliability, or manufacturability of its products. Before placing an order, the user is cautioned to verify that the information being relied upon is current.

Allegro's products are not to be used in any devices or systems, including but not limited to life support devices or systems, in which a failure of Allegro's product can reasonably be expected to cause bodily harm.

The information included herein is believed to be accurate and reliable. However, Allegro MicroSystems assumes no responsibility for its use; nor for any infringement of patents or other rights of third parties which may result from its use.

Copies of this document are considered uncontrolled documents.

For the latest version of this document, visit our website:

www.allegromicro.com